BIOLOGY, MEDICINE, & NATURAL PRODUCT CHEMISTRY ISSN 2089-6514 (paper)
Volume 15, Number 1, April 2026 | Pages: 1321-1327 | DOI: 10.14421/biomedich.2026.151.1321-1327 ISSN 2540-9328 (online)

Metabolomics-Based Profiling of Antioxidant Compounds in Kesum (*Polygonum minus*) via UHPLC-Q-Orbitrap HRMS as Potential Anti-SARS-CoV-2 Candidates: An In Silico Approach

Iche Azani, Dini Hadiarti*, Arni, Nur Aulia Fitri
Chemistry Education Study Program, Universitas Muhammadiyah Pontianak, Kalimantan Barat
Jl. A Yani No. 111, Pontianak, 78124, Indonesia.

Corresponding author*
dinihadiarti@unmuhpnk.ac.id

Manuscript received: 13 February 2026. Revision accepted: 20 June 2026, Published: 09 July 2026.

Abstract

Kesum or *Polygonum minus* (*P. minus*) is well-known for its high antioxidant content and potential as a therapeutic agent. This study aimed to identify active compounds in P. minus leaf extracts that serve as antioxidants and SARS-CoV-2 inhibitor candidates using metabolomics approach. *P. minus* leaves were extracted with ethanol and subsequently fractionated using n-hexane, ethyl acetate, and water. The ethyl acetate fraction exhibited the highest antioxidant activity as measured by the DPPH method. Further analysis using UHPLC-Q-Orbitrap HRMS identified several compounds, including 3-hydroxybenzoic acid, quercetin-3β-D-glucoside, tectoridin, apigenin, hispidulin, and (±)-usnic acid. These compounds were subsequently evaluated in silico by molecular docking against the 1OG5 and 7CMD target proteins. The results demonstrated strong interactions between these compounds and the protein active sites, supporting their potential as both antioxidants and inhibitors of SARS-CoV-2. This study suggests that P. minus is a promising source of bioactive compounds for development in herbal-based therapies in West Kalimantan.

Keywords: Antioxidant; *Polygonum minus*; metabolomic; UHPLC-Q-Orbitrap HRMS; SARS-CoV-2; *molecular docking*.

INTRODUCTION

The World Health Organization (WHO) reported more than 779 million confirmed COVID-19 cases globally, resulting in over 7.1 million deaths as of January 18, 2026. In Indonesia, confirmed cases have exceeded 6.8 million, with a mortality toll reaching over 162,000 since January 3, 2020, through January 18, 2026 (WHO, 2026). The COVID-19 virus accelerates oxidation reactions driven by free radicals within the body, leading to respiratory distress syndromes. Antioxidants possess the capacity to suppress the levels of reactive oxygen species (ROS), a property notably found in *Polygonum minus*.

P. minus leaves, commonly known as Kesum, have been proven to function as antioxidants. Flavonoids, phenolics, alkaloids, tannins, and saponins present in the methanol, ethanol, aqueous, and ethyl acetate extracts of *P. minus* leaves are estimated to be responsible for their antioxidant activity (Wibowo et al., 2013; Christapher et al., 2014; George et al., 2014; Ghazali et al., 2014; Elatior, Mavaddat, and Ali, 2015; Abdullah et al., 2017; Purwaningsih and Sapriani, 2018; Muthukumarasamy et al., 2018; Hamid et al., 2020). Identification of the methanolic extract of P. minus leaves using LCMS-IT-TOF revealed the presence of apigenin, hyperoside, isoquercetin, astragalin, miquelianin, quercetin, and quercitrin (Abdullah et al., 2017).

An investigation into the antioxidant activities of the compounds identified by Abdullah et al. (2017) using both in vitro and in silico approaches has not yet been conducted. The determination of secondary metabolites and functional groups that significantly influence antioxidant activity can be enabled through a metabolomics approach. The determination of secondary metabolites and functional groups that predominantly influence antioxidant activity has been streamlined through an FTIR-based metabolomics approach in extracts of *Syzygium polyanthum* (Rohaeti, Karunina, and Rafi, 2021), *Curculigo orchioides*, and *C. latifolia* (Umar et al., 2021). Furthermore, the profiling of antioxidant compounds using UHPLC-Q-Orbitrap HRMS has been demonstrated in extracts of *Cannabis sativa* (Izzo et al., 2020), *C. orchioides*, and *C. latifolia* (Umar et al., 2021). Additionally, the antioxidant activities of compounds identified from *Malva sylvestris* (Irfan et al., 2021) and *Zinnia elegans* (Samy et al., 2022) have been evaluated through molecular docking.

The urgency of discovering active compounds from *P. minus* leaf extract coincides with the continuous

evolution of COVID-19, necessitating antioxidants capable of slowing free radical-induced oxidation alongside potential inhibitors. In this study, *P. minus* leaves were macerated in ethanol and subsequently fractionated with n-hexane, ethyl acetate, and water. All resulting extracts and fractions were evaluated for their antioxidant activity, Total Phenolic Content (TPC), and Total Flavonoid Content (TFC), followed by FTIR spectroscopy analysis. Multivariate analysis, including Principal Component Analysis (PCA) and Partial Least Squares (PLS) regression, was also performed. The fraction exhibiting the highest antioxidant activity was further analyzed via UHPLC-Q-Orbitrap HRMS to identify its active compounds. The identified chemical structures were then subjected to in silico antioxidant and COVID-19 inhibitory assays through molecular docking against the target proteins Human Cytochrome P450 CYP2C9 (PDB ID: 1OG5) and SARS-CoV-2 Papain-Like Protease (PLpro) (PDB ID: 7CMD). This research aims to explore the potential of active compounds from *P. minus* leaves as antioxidants and COVID-19 inhibitor candidates, with a focus on identifying bioactive compounds and analyzing inhibitory mechanisms through a metabolomics approach.

MATERIALS AND METHODS

Maceration and Fractionation

P. minus leaves were sourced from Ketapang Regency, West Kalimantan, and authenticated by a botanist at the Department of Biological Education of Universitas Muhammadiyah Pontianak. A total of 15 kilogram of *P. minus* leaves were cleaned and air-dried at room temperature for 7 days. The dried leaves were pulverized and macerated in ethanol for 3 days, with the solvent being refreshed daily. The resulting macerate was filtered and evaporated at 40 °C until no more solvent dripped. Fractionation was conducted using liquid-liquid extraction with solvents of increasing polarity: n-hexane, ethyl acetate, and water. The resulting fractions were filtered, evaporated under reduced pressure, and stored in a refrigerator at -4 °C.

Phytochemical Screening

Phytochemical screening of alkaloids, flavonoids, phenolics, steroids, triterpenoids, saponins, and tannins in *Polygonum minus* leaf extracts and fractions was conducted according to the method of Rubianti et al. (2022). The study was carried out at the Laboratory of Universitas Muhamamdiyah Pontianak in 2023 using standard laboratory equipment. The materials used included ethanol, NaOH, HCl, H_2SO_4, chloroform, $FeCl_3$, dragendorff's reagent, mayer's reagent, and distilled water.

In Vitro Antioxidant Activity Assay (DPPH)

The antioxidant activity was analysed by mixing 100 µL of the *P. minus* extract or fraction with 0.5 mL of DPPH solution. The DPPH stock solution was prepared by dissolving 4 mg of DPPH in 10 mL of ethanol, with its absorbance measured at 517 nm. The mixture was incubated at 37 °C for 30 minutes, and the final absorbance was recorded at 517 nm using a UV-Vis spectrophotometer (Izzo et al., 2020; Umar et al., 2021).

FTIR Spectroscopy Analysis

Fourier Transform Infrared (FTIR) analysis was performed using a Shimadzu IRPrestige-21 spectrophotometer (Tokyo, Japan) at the Organic Chemistry Laboratory, Universitas Gadjah Mada, in 2023. Samples were prepared by mixing 2 mg of extract or fraction with 180 mg of KBr and compressing the mixture into pellets under 8 tons of pressure for 15 min. Spectra were recorded in the range of 4000–400 cm^{-1} at a resolution of 4 cm^{-1} with 45 scans min^{-1}. All measurements were performed in triplicate to ensure reproducibility (Umar et al., 2021).

Total Flavonoids and Phenolics Content Analysis

The determination of total flavonoid content (TFC) and total phenolic content (TPC) was conducted at the Biofarmaka, Institut Pertanian Bogor, in 2023. TFC was analyzed using the aluminum chloride ($AlCl_3$) colorimetric method with quercetin as the reference standard and measured at a wavelength of 436 nm using a UV–Vis spectrophotometer. TPC was determined using the Folin–Ciocalteu method with gallic acid as the standard and measured at 701 nm. The results were expressed as quercetin equivalents (QE) and gallic acid equivalents (GAE) per 100 g of extract, respectively (Hadiarti et al., 2021).

Identification of Compounds Using UHPLC-Q-Orbitrap HRMS

Approximately 50 mg of ethyl acetate extract was ultrasonicated with 1.5 mL of methanol at 30 ºC for 15 minutes. The mixture was filtered through a P TFE membrane filter (SY25TF, mdi) and transferred into a vial. Compound identification was performed using a Vanquish Flex UHPLC-Q Exactive Plus Orbitrap High-Resolution Mass Spectrometer equipped with an Accucore™ Phenyl Hexyl column (100 × 2.1 mm, 2.6 µm) and a UV detector set at 254 nm. Mass analysis was conducted using electrospray ionization (ESI) coupled with a Q-Orbitrap analyzer. The mobile phase consisted of 0.1% formic acid in water (A) and 0.1% formic acid Orbitrap analyzer. The mobile phase consisted of 0.1% formic acid in water (A) and 0.1% formic acid in acetonitrile (B) under the following gradient conditions: 0.00–1.73 min (30–40% B), 1.73–6.93 min (40–75% B), 6.93–7.80 min (75–100% B), 7.80–8.23 min (100–30% B), and 8.23–13.00 min (30% B). The flow rate was 0.2 mL min^{-1}, and the injection volume was 2 µL. Data processing, including spectrum selection, retention time alignment, and database matching, was carried out using

Compound Discoverer version 2.2 (Rafi et al., 2021; Umar et al., 2021).

The Molecular Docking

The identified metabolites from UHPLC-Q-Orbitrap HRMS were subjected to *in silico* molecular docking analysis. The three-dimensional (3D) structures of these compounds were either retrieved from the PubChem database or modeled using ChemDraw Professional 17.1. The crystal structures of the target proteins, 2QMJ and 3TOP, were obtained from the Protein Data Bank (PDB). Ligand and protein preparation, including the removal of solvent molecules and the addition of necessary charges, was performed using UCSF Chimera 1.14. Docking simulations were executed using AutoDock 4.2.6 (via AutoDockTools 1.5.6) on a Windows 10 platform. A grid box of 60 × 60 × 60 Å with a spacing of 0.375 Å was centered on the active sites of the proteins. The docking parameters employed the Lamarckian Genetic Algorithm (LGA) with a maximum of 2,500,000 energy evaluations, 27,000 generations, a mutation rate of 0.02, a population size of 150, and 100 runs. The resulting docking poses were evaluated based on the lowest binding energy and inhibition constant (Ki). Finally, the ligand-protein intermolecular interactions were visualized and analyzed using Discovery Studio Visualizer (Farooq et al., 2020; Nadeem et al., 2020).

RESULTS AND DISCUSSION

Extraction Yield, Phytochemical, and Antioxidant Activity

The extraction of *P. minus* yielded higher amounts of ethanol and aqueous extracts compared to the n-hexane and ethyl acetate fractions, as shown in Table 1. This indicates that *P. minus* contains a higher proportion of polar compounds relative to non-polar and semi-polar constituents. Phytochemical screening confirmed the presence of flavonoids and phenolics across all extracts. The TFC was highest in the ethanol fraction, whereas the TPC reached its peak in the ethyl acetate fraction. Notably, the ethyl acetate fraction exhibited the lowest IC_{50} value, categorizing its antioxidant activity as very strong (Souhoka et al., 2019). These results clearly demonstrate that semi-polar solvents are the most effective in extracting antioxidant compounds. Given that the ethyl acetate fraction possessed the highest TPC, it is highly probable that phenolic compounds are the primary contributors to the antioxidant activity. This finding is consistent with previous studies, which reported that extracts with the highest TPC often exhibit superior antioxidant potential (Aryal et al., 2019; Deseo et al., 2020; Motsumi et al., 2020).

Table 1. Extraction Yield TPC, TFC, and IC_{50} Values of *P. Minus* Extracts.

Sample	Yield (%)	TPC (g GAE/100 g extract)	TFC (g QE/100 g extract)	IC_{50} Antioxidant (mg/L)
Ethanol	9	4,25	189,83	21,09
n-Hexane	0,7	11,04	11,04	inactive
Ethyl Acetate	0,5	16,77	160,3	15,35
Water	1,2	1,71	78,81	24,02

Correlation of Functional Group to Extract and Antioxidant Activity

The FTIR spectra shown in Figure 1 and Table 2 illustrate the functional groups present in *P. minus* leaves extracts within the mid-infrared region (4000–400 cm^{-1}). The ethyl acetate fraction exhibited the highest absorption intensity compared to the other extracts. While all four extracts and fractions displayed similar spectral patterns, their absorption intensities varied significantly. Differences in absorbance intensity were observed for the -OH group at wavenumbers 3394–3410 cm^{-1}, with the highest value recorded in the ethyl acetate extract. Furthermore, the ethyl acetate fraction showed higher intensity for the C=C (alkene) group, typically absorbing in the range 1680–1600 cm^{-1}, relative to other samples.

PCA analysis of the FTIR results (Figure 2) indicated that the functional groups in the ethanol extract, ethyl acetate fraction, and aqueous fraction did not differ substantially. This similarity is attributed to the polar and semi-polar nature of these solvents, which selectively extract compounds with corresponding polarities. Furthermore, the PLS plot (Figure 3) revealed that the functional groups significantly influencing antioxidant activity are the -OH groups from phenolic and aromatic compounds.

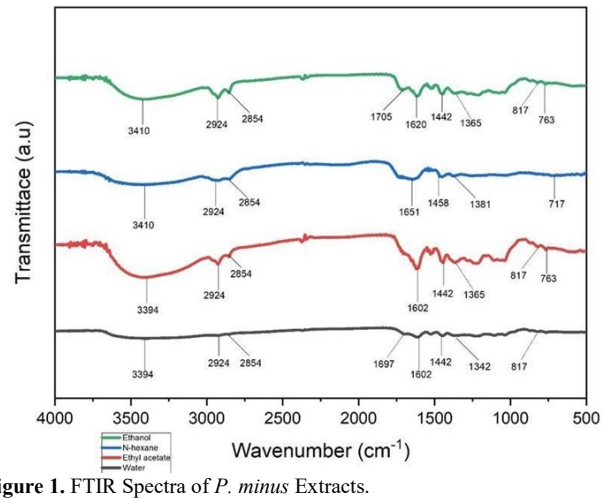

Figure 1. FTIR Spectra of *P. minus* Extracts.

Table 2. Identified Functional Groups of *Polygonum minus* Extract.

Wavenumber (cm^{-1})	Detected Wavenumber (cm−1)	Functional Groups	Vibration Mode	Peak Code	Et1	Et2	Et3	Xe1	Xe2	Xe3	Ea1	Ea2	Ea3	Wt1	Wt2	Wt3
2990 -2850	2924	C-H Alkanes	Stretching	**A**	√	√	√	√	√	√	√	√	√	√	√	√
1450-1375	1442, 1450, 1458	-CH_3	Bending	**B**	√	√	√	√	√	√	√	√	√	√	√	√
1680-1600	1604, 1651, 1620, 1635	C=C Alkenes	**Stretching**	**C**	√	√	√	√	√	√	√	√	√	√	√	√
1625-1440	1527, 1512, 1519	C=C Aromatic	**Stretching**	**D**	√	√	√				√	√	√	√	√	√
3550-3200	3394, 3410,	O-H	**Stretching**	**E**	√	√	√	√	√	√	√	√	√	√	√	√
2900-2800	2854	C-H Aldehydes	**Stretching**	**F**	√	√	√	√	√	√	√	√	√	√	√	√
1715-1680	1697, 1705	C=O	**Stretching**	**G**	√	√		√			√		√	√	√	
1390-1310	1342, 1365, 1381, 1373	O-H Phenol	**Bending**	**H**	√	√	√	√	√	√	√	√	√	√	√	√
1260-1050	1226, 1219, 1249, 1257, 1242, 1211,	C-O Ether	**Stretching**	**I**	√	√	√	√	√	√	√	√	√	√	√	√
720-680	717		**Bending**	**J**					√							
770 – 735	763		**Bending**	**K**	√	√					√	√		√	√	√
860 – 800	817	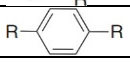	**Bending**	**L**	√	√					√	√	√		√	√

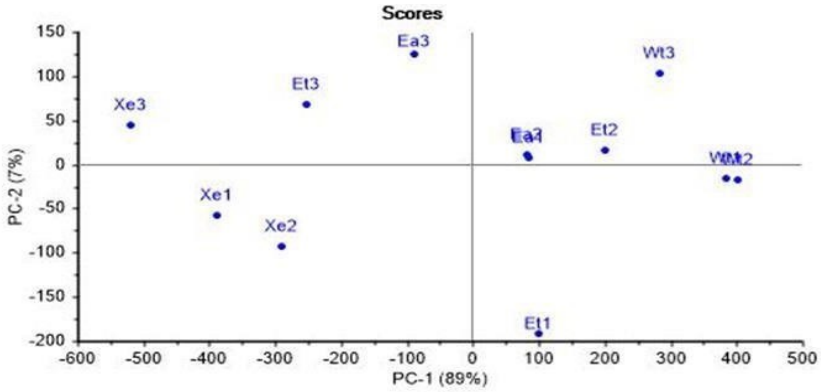

Figure 2. PCA Plot of Functional Group from *P.minus* Extract based on FTIR Results.

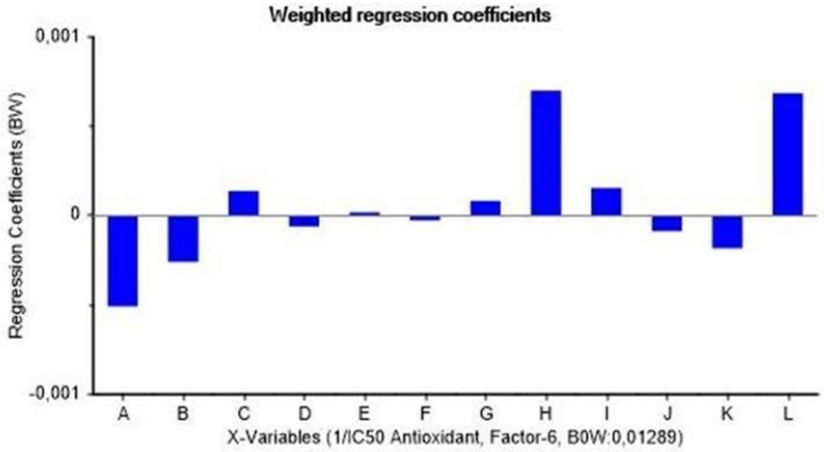

Figure 3. Plot Standardization Coefficient of *P. minus* Extract.

Profile of Flavonoid and Phenolic

The ethyl acetate fraction was subjected to UHPLC-Q-Orbitrap HRMS analysis to characterize its antioxidant constituents. Adhering to a mass accuracy criterion of < 5 ppm, six phenolic and flavonoid compounds were identified (Table 3). Compounds such as 3-

hydroxybenzoic acid (Korkmaz et al., 2019) and (±)-usnic acid (Maulidiyah et al., 2021) were identified, both of which are documented antioxidants. The flavonoid profile included hispidulin (Ren et al., 2019; Vanessa et al., 2023) and apigenin (Aisya et al., 2024; Wati et al., 2025; Barut and Demir, 2019), which are well-known for their free radical scavenging capacities. Additionally, the identification of tectoridin (Sudradjat et al., 2022) and quercetin-3β-D-glucoside (Korkmaz et al., 2019; Wati et al., 2025; Barut and Demir, 2019) supports the strong antioxidant potential of the fraction. This comparative literature analysis confirms that these identified metabolites serve as the bioactive markers for the antioxidant properties of the *P. minus* ethyl acetate fraction.

Table 3. Identification of Compounds from the Ethyl Acetate Fraction of *P. minus* Using UHPLC-Q-Orbitrap HRMS.

Sample	Retention Time (menit)	Molecular Formula	Theoretical Mass (m/z)	Experimental Mass (m/z)	Accuracy Mass (ppm)	[M-H]-/[M+H]+	Reference
3-Hydroxy benzoic acid	5.501	C7H6O3	187.024265	138.03158	-261958.9763	137.02364	PubChem
Quercetin-3β-Dglucoside	8.776	C21H20O12	464.09548	464.09638	1.93925612	463.088 44	PubChem
Tectoridin	11.925	C22H22O11	462.116215	462.11738	2.521010867	461.109 44	PubChem
Apigenin	12.682	C15H10O5	270.052825	270.05372	3.314166404	269.045 78	PubChem
Hispidulin	12.878	C16H12O6	300.06339	300.06434	3.165997691	299.056 4	PubChem
(.+/-.)-Usnic acid	16.841	C18H1607	344.089605	344.09049	2.572004464	343.082 55	PubChem

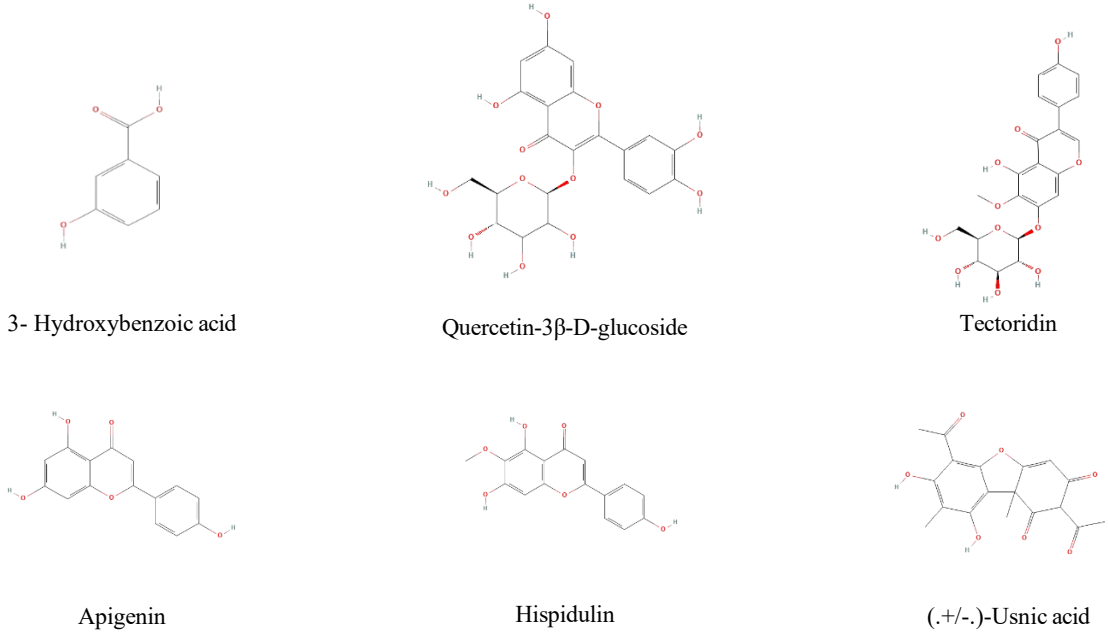

Figure 4. Identified Compounds from the Ethyl acetate Fraction of *P. minus.*

Molecular Docking Study

The identified compounds were further docked with the 1OG5 and 7CMD proteins to assess their potential as antioxidants and anti-COVID-19 agents. These proteins were selected due to their higher resolution compared to other available structures. The molecular docking results are presented in Table 4. Figure 5 shows that the Hispidulin-1OG5 and Quercetin-3β-D-glucoside-7CMD complexes exhibited the lowest binding energies, demonstrating greater binding affinity compared to ascorbic acid, which was used as the control ligand.

Table 4. Molecular Docking Analysis of identified Compounds from P. minus Ethyl acetate Fraction Against Antioxidant and COVID-19 Proteins.

Compounds	Protein	$\Delta G_{binding}$ (kcal/mol)	Ki (μM)	Hydrogen Bonds
Ascorbic Acid (Control Ligand)	7CMD	-4,64	399,55	ASP164, **ARG166**, SER245, and ASO302
	1OG5	-2,67	10.960	PHF00, ALA103, ASN217, and GLN214
Hispidulin	7CMD	-3,76	1.750	LYS291, GLU280, HIS255
	1OG5	-8,41	0,67973	ASN133, PHE419,dan SER343
Apigenin	7CAM	-8,06	1,23	LEU141
	1OG5	-8,39	0,71275	THR305, GLN356, dan LEU361
Tectoridin	7CMD	-4,91	249,7	GLY266, GLN269, and LEU162

Compounds	Protein	$\Delta G_{binding}$ (kcal/mol)	Ki (µM)	Hydrogen Bonds
	1OG5	-5,48	96,22	LEU208, PHE476, PHE100, and GLY98
Quercetin-3β-D-glucoside	**7CMD**	**-8,30**	**0,826**	**ARG166, THR301, GLY266, and TYR264**
	1OG5	-4,14	929,89	SER209, ASN474, GLU206, and TRP212
3-Hydroxybenzoic acid	7CMD	-3,57	2140	GLN269 and TYR273
	1OG5	-3,25	2640	PHE100
(.+/-.)-Usnic acid	7CMD	-6,87	9,27	GLN269
	1OG5	-6,02	38,82	PHE476

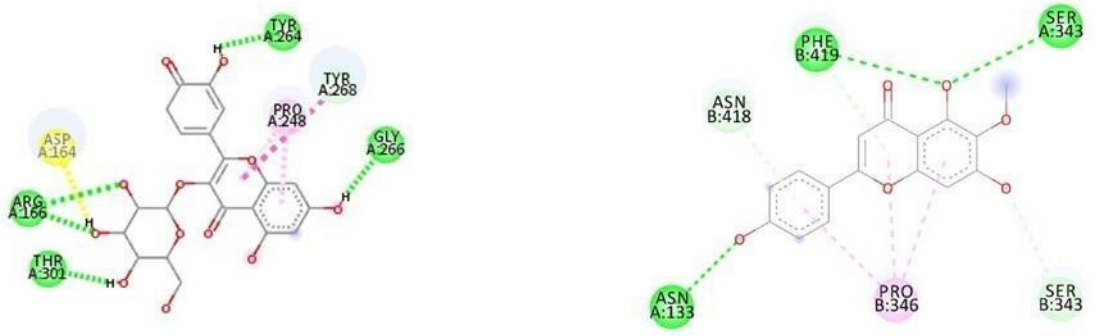

Complex of Hispidulin-1OG5 Complex Quercetin-3β-D-glucoside-7CMD

Figure 5. Interaction of Hispidulin with 1OG5 and Quercetin-3β-D-glucoside with 7CMD.

CONCLUSIONS

This study successfully identified bioactive compounds from the leaf extract of *Polygonum minus* (kesum) exhibiting potent antioxidant activity and promising SARS-CoV-2 inhibitory potential through a combined metabolomics and in silico approach. The ethyl acetate fraction demonstrated the highest antioxidant capacity, which correlated with its superior phenolic content, significantly contributing to its radical scavenging ability. Identification via UHPLC-Q-Orbitrap HRMS revealed the presence of key phenolic and flavonoid constituents, namely 3-hydroxybenzoic acid, quercetin-3β-D-glucoside, tectoridin, apigenin, hispidulin, and (±)-usnic acid. Molecular docking simulations further indicated that hispidulin and quercetin-3β-D-glucoside possess high binding affinities toward target proteins 1OG5 and 7CMD, respectively, suggesting their potential roles as antioxidant and antiviral agents. Consequently, P. minus holds significant potential for further development as a natural source for managing oxidative stress and as a supportive therapeutic candidate for COVID-19.

Acknowledgements: The authors are grateful to the Ministry of Education, Culture, Research, and Technology (Kemendikbudristek) for the financial support provided under the Program Kreativitas Mahasiswa-Riset Eksakta (PKM-RE) fiscal year 2023, in accordance with the Decree Number 2383/E2/DT.01.00/2023.

Competing Interests: The authors declare that there are no competing interests.

REFERENCES

Arrebola-Liébanas, F. J., Romero-González, R. and Garrido Frenich, A. (2017) 'HRMS: Fundamentals and Basic Concepts', in Romero-González, R. and Frenich, A. G. (eds) Applications in High Resolution Mass Spectrometry: Food Safety and Pesticide Residue Analysis. 1st edn. Amsterdam: Elsevier Inc, pp. 1–14. doi: 10.1016/B978-0-12-809464-8.00001-4.

Avogaro, A. and Fadini, G. P. (2014) 'The effects of dipeptidyl peptidase-4 inhibition on microvascular diabetes complications', Diabetes Care, 37(10), pp. 2884–2894. doi: 10.2337/dc14-0865.

Dewi, N. S. A. and Sanjaya, I. G. M. (2018) 'Study Komputasi Aktivitas Senyawa Turunan Mangiferin Sebagai Anti Diabetes Tipe 1 Menggunakan Metode Hksa (Hubungan Kuantitatif Struktur Dan Aktivitas) Dan Penambatan Molekulcomputational Study of Mangiferin Compound and Its Derivate As an Anti Diabetic T', Unesa Journal of Chemistry, 7(1), pp. 8–14.

Dysted, M. P. et al. (2021) IDF Diabetes Atlas. 10th edn, Diabetes Research and Clinical Practice. 10th edn. Edited by E. J. Boyko et al. Bruessel: International Diabetes Federation. doi: 10.1016/j.diabres.2013.10.013.

Farooq, M. U. et al. (2020) 'UHPLC-QTOF-MS/MS based phytochemical characterization and anti-hyperglycemic prospective of hydro-ethanolic leaf extract of Butea monosperma', Scientific Reports, 10(1), pp. 1–15. doi: 10.1038/s41598-020-60076-5.

Freitas, R. F. De and Schapira, M. (2017) 'A systematic analysis of atomic protein – ligand interactions in the PDB †', MedChemComm, 8(10), pp. 1970–1981. doi: 10.1039/c7md00381a.

García-Reyes, J. F. et al. (2017) 'HRMS: Hardware and Software', in Romero- González, R. and Frenich, A. G. (eds) Applications in High Resolution Mass Spectrometry: Food Safety and Pesticide Residue Analysis. 1st edn. Amsterdam: Elsevier Inc., pp. 15–57. doi: 10.1016/B978-0-12-809464- 8.00002-6.

Hadiarti, D. et al. (2021) 'UNDERSTANDING PHYTOCHEMICAL ROLES ON α-GLUCOSIDASE INHIBITORY ACTIVITY BASED ON METABOLOMIC APPROACH OF Premna serratifolia LEAVES FROM WEST BORNEO, INDONESIA', Rasayan Journal of Chemistry, 14(02), pp. 1216–1222. doi: 10.31788/rjc.2021.1426320.

Holdgate, G. A., Meek, T. D. and Grimley, R. L. (2018) 'Mechanistic enzymology in drug discovery: A fresh perspective', Nature Reviews Drug Discovery, 17(2), pp. 115–132. doi: 10.1038/nrd.2017.219.

Kurniawan, M. F. et al. (2017) 'Metabolomic approach for understanding phenolic compounds and melanoidin roles on antioxidant activity of Indonesia robusta and arabica coffee extracts', Food Science and Biotechnology, 26(6), pp. 1475–1480. doi: 10.1007/s10068-017-0228-6.

Li, Q. et al. (2016) 'Chemical constituents and quality control of two Dracocephalum species based on high-performance liquid chromatographic fingerprints coupled with tandem mass spectrometry and chemometrics', Journal of Separation Science, 39(21), pp. 1–15. doi: 10.1002/jssc.201600645.

Lopina, O. D. (2016) 'Enzyme Inhibitors and Activators', in Senturk, M. (ed.) Enzyme Inhibitors and Activators. IntechOpen, p. 13.

Murugesu, S. et al. (2018) 'Characterization of α-glucosidase inhibitors from clinacanthus nutans lindau leaves by gas chromatography-mass spectrometry- based metabolomics and molecular docking simulation', Molecules, 23(9), pp. 1–21. doi: 10.3390/molecules23092402.

Nadeem, M. et al. (2020) 'Antidiabetic functionality of Vitex negundo L. leaves based on UHPLC-QTOF-MS/MS based bioactives profiling and molecular docking insights', Industrial Crops and Products, 152(May), p. 112445. doi: 10.1016/j.indcrop.2020.112445.

Nokhala, A. et al. (2020) 'Characterization of α-glucosidase inhibitory activity of Tetracera scandens leaves by Fourier transform infrared spectroscopy-based metabolomics', Advances in Traditional Medicine, 20(2), pp. 169–180. doi: 10.1007/s13596-019-00417-6.

Rafi, M. et al. (2021) 'Inhibition of α-glucosidase activity, metals content, and phytochemical profiling of Andrographis paniculata from different geographical origins based on FTIR and UHPLC-Q-Orbitrap HRMS metabolomics', Biodiversitas, 22(3), pp. 1535–1542. doi: 10.13057/BIODIV/D220359.

Ramsay, R. R. and Tipton, K. F. (2017) 'Assessment of enzyme inhibition: A review with examples from the development of monoamine oxidase and cholinesterase inhibitory drugs', molecules, 22(1192), pp. 1–47. doi: 10.3390/molecules22071192.

Rouzbehan, S. et al. (2017) 'Kinetics of α-glucosidase inhibition by different fractions of three species of Labiatae extracts: A new diabetes treatment model', Pharmaceutical Biology, 55(1), pp. 1483–1488. doi: 10.1080/13880209.2017.1306569.

Rubianti, I., Azmin, N. and Nasir, M. (2022) 'Analisis Skrining Fitokimia Ekstrak Etanol Daun Golka (Ageratum conyziodes) Sebagai Tumbuhan Obat Tradisional Masyarakat Bima', JUSTER: Jurnal Sains dan Terapan, 1(2), pp. 7–12. doi: 10.55784/juster.v1i2.67.

Trygg, J. and Wold, S. (2002) 'Orthogonal projections to latent structures (O-PLS)',

Journal of Chemometrics, 16(3), pp. 119–128. doi: 10.1002/cem.695.

Umar, A. H. et al. (2021) 'Untargeted metabolomics analysis using ftir and uhplc- q-orbitrap hrms of two curculigo species and evaluation of their antioxidant and α-glucosidase inhibitory activities', Metabolites, 11(1), pp. 1–17. doi: 10.3390/metabo11010042.

Wibowo, M. A., Ferdinan, A. and Idiawati, N. (2015) 'AKTIVITAS ANTIDIABET FRAKSI N-HEKSANA DAUN KESUM (*Polygonum minus*)', in Prosiding Simposium Nasional Kimia Bahan Alam ke-23 (SimnasKBA-2015), pp. 168– 171.

THIS PAGE INTENTIONALLY LEFT BLANK